A Comparative Analysis of Monte Carlo Reference and Two-Step Diffusion Solution for a Soluble-Boron-Free i-SMR Core

Dongju Choi [a], Yunseok Jeong [a], Yonghee Kim [a*]
[a]*Department of Nuclear and Quantum Engineering, KAIST*
[*]*Corresponding author: yongheekim@kaist.ac.kr*

Keywords: i-SMR, HIGA, Serpent, KANT

1. Introduction

The establishment of a reference solution is crucial for ensuring the theoretical validity and methodological reliability of reactor core analysis. The Monte Carlo method provides the highest accuracy by explicitly representing neutron transport in a continuous energy spectrum while preserving reactor geometry. However, whole-core calculations are computationally prohibitive due to excessive memory and time requirements.

The two-step method mitigates this limitation by balancing accuracy and efficiency. It first evaluates neutron behavior at a local level with high fidelity before projecting it onto a macroscopic framework. Spatial homogenization and energy condensation simplify the physics while preserving essential neutron transport characteristics at the core level. Although the two-step method is a practical alternative, its accuracy relies on the fidelity of homogenization and discontinuity factors.

This study establishes a Monte Carlo whole-core reference solution and compares it with a two-step diffusion solution. The analysis focuses on Soluble-Boron-Free i-SMR core featuring Highly Intensive and Discrete Gadolinia/Alumina [1] as a burnable absorber. The reference solution is calculated using the Serpent Monte Carlo code [2] and evaluated against the 3D nodal diffusion code KANT (KAIST Advanced Nuclear Tachygraphy) [3].

2. Methods

2.1 Monte Carlo-based whole-core calculation

Since whole-core Monte Carlo calculations are computationally prohibitive, a quarter-core model is adopted to balance accuracy and efficiency. Initially, fuel assemblies are modeled assembly-wise, where all fuel rods share the same depletion history. While efficient, this approach cannot capture fine intra-assembly spectral variations and localized burnup effects of burnable absorbers.

Highly Intensive and Discrete Gadolinia/Alumina (HIGA), a non-fuel rod burnable absorber, exhibits pronounced self-shielding. Figure 1 presents the absorption reaction rates and number density of Gd-155 and Gd-157 within HIGA rods inside the fuel assembly, highlighting radial variations among the inner, middle, and outer regions. These variations result from neutron flux depression and strong self-shielding effects. To accurately capture this behavior, HIGA is independently depleted using pin-wise modeling.

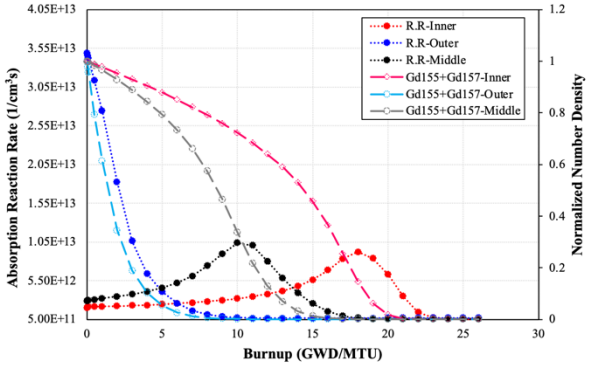

Figure 1. Radial variations in absorption reaction rate and number densities of Gd-155 and 157 in HIGA

Also, fuel rod grouping is adopted as a practical alternative to reduce the computational burden of fully pin-wise depletion. A 3×3 and 9×9 grouping is used, where rods within each subregion share depletion history. Figure 2 compares the different fuel assembly configurations.

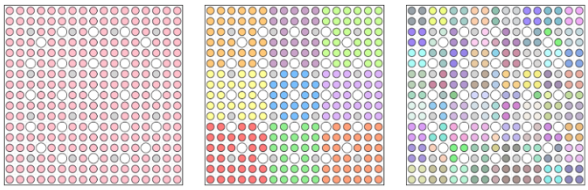

Figure 2. Fuel assembly configurations: (left) assembly-wise, (center) 3×3 grouping, (right) 9×9 grouping.

Pin-wise depletion is performed with domain decomposition to optimize computational efficiency. By dividing the core into subdomains, it enables localized pin-wise depletion while reducing memory usage and computational time. Figure 3 illustrates the reactor core layout and the application of domain decomposition for preserving spectral and spatial fidelity.

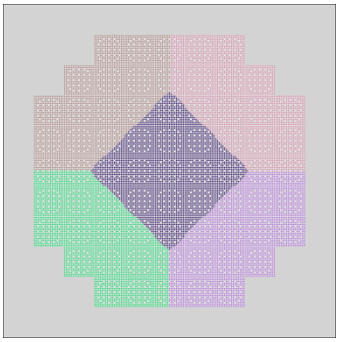

Figure 3. Domain decomposition of the i-SMR core

2.2 Two-step analysis

Homogenized group constants (HGC) were generated using the Serpent2 Monte Carlo code, ensuring higher fidelity than deterministic methods by fully accounting for continuous energy neutron transport. To accurately model the depletion behavior of HIGA, a sufficiently small burnup step was applied for HGC generation. Figure 4 illustrates the effect of burnup step size on reactivity behavior, emphasizing the need for fine steps.

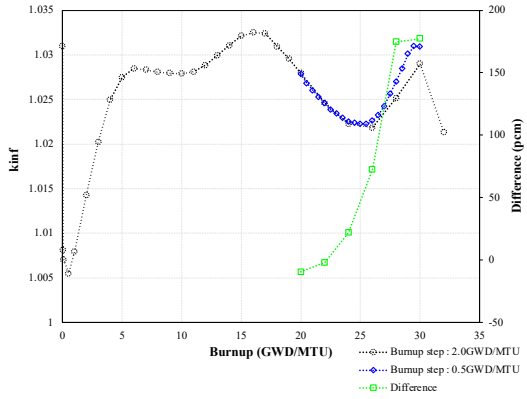

Figure 4. HIGA fuel assembly depletion behavior

For discontinuity factors, assembly discontinuity factors (ADF) were applied based on the Simplified Equivalence Theory (SET). Axial reflector DFs were determined using a 1-D spectral geometry. For radial reflectors, DFs were obtained from two different modeling approaches. The conventional spectral geometry employed a 1D model for I-shape reflectors and a 2D model for L-shape reflectors. In contrast, a 2D quarter-core model was used to obtain a higher-fidelity reference DF. Since KANT is based on NEM-CMFD, the DFs were also generated by NEM calculations.

Figure 5 shows spectral geometry and 2D whole-core model for radial reflectors, while Figure 6 shows the spectral geometry for axial reflector.

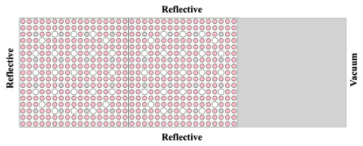

(a) Spectral geometry for i-shape reflector

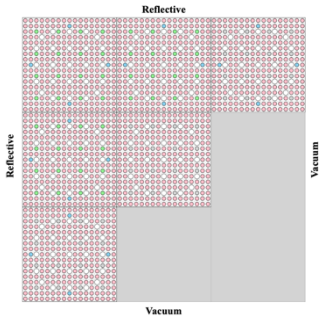

(b) Spectral geometry for L-shape reflector

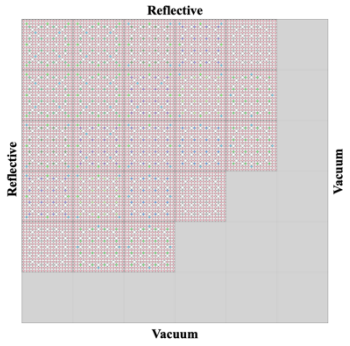

(c) 2D quarter core

Figure 5. Spectral geometries for radial reflector: (a) 1D i-shape, (b) 2D L-shape, and (c) 2D quarter core

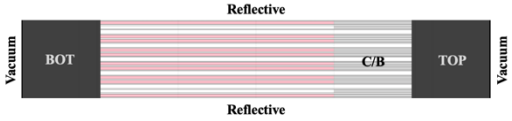

Figure 6. Spectral geometry for Axial reflector

3. Numerical Results

3.1 Monte Carlo reference solution

To ensure accurate depletion modeling for HIGA, the predictor-corrector scheme was first evaluated. Isotalo [4] observed that linear interpolation in the corrector step can lead to error cancellation, potentially improving accurac, and emphasized the need for additional studies to determine whether linear or quadratic interpolation is more appropriate, particularly for PWR assemblies with gadolinia. Given these considerations both LELI and LEQI methods were tested under identical conditions. The reference solution was generated with 524 depletion steps of 0.05 GWD/MTU, maintaining a 1σ uncertainty of 5 pcm.

Figure 7 compares the two methods, showing that LELI exhibited smaller deviations, leading to its selection for this study.

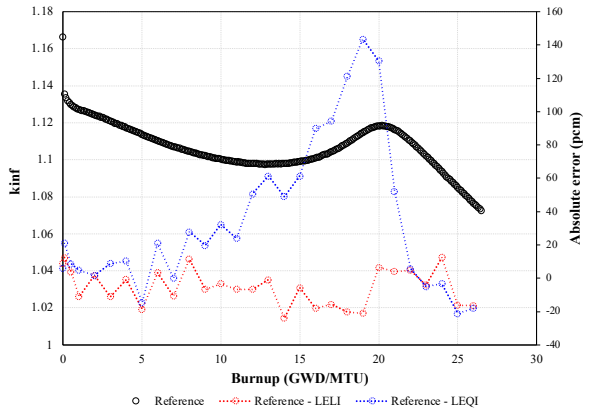

Figure 7. Comparison of LELI and LEQI predictor-corrector scheme for HIGA fuel assembly depletion.

Whole-core depletion calculations were performed using the CRAM depletion solver with the predictor-corrector LELI method. All burnable absorbers, including HIGA, were depleted in a fully pin-wise manner to consider the self-shielding effects. Figure 8 presents the reactivity over EFPD, illustrating the impact of spatial modeling approaches on reactivity behavior. As burnup progresses, discrepancies between the modeling approaches become more pronounced, with the assembly-wise model showing the largest deviation from the pin-wise reference. Around 200 pcm difference is observed at higher burnup levels, with fuel-grouped models showing intermediate behavior between the two extremes. This highlights the importance of detailed fuel modeling for accurate depletion calculations.

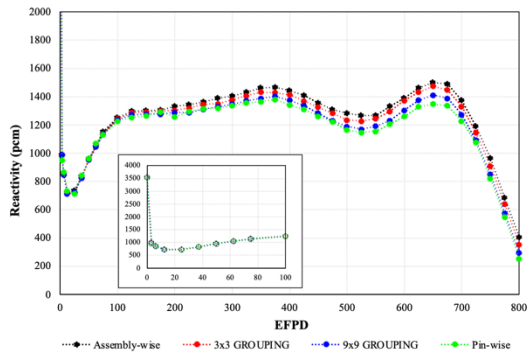

Figure 8. Reactivity comparison for different fuel rod modeling in whole-core depletion

Additionally, depletion conditions and computational requirements are summarized in Table 1.

Table 1. Depletion conditions and computational requirements

	Assembly-wise	3x3 Grouping	9x9 Grouping	Pin-wise
History	2.00E+06	2.00E+06	2.00E+06	5.00E+05
Active/Inactive	300/100	300/100	300/100	300/100
Uncertainty (pcm)	5	5	5	10
Computing times (hour)	35.2	61.3	79.3	92.9
Memory use (GB/node)	96	142	325	384

3.2 Two-step diffusion solution

Table 2 compares the flux and DF values at the reflector-fuel interface for the L-shape reflector, as the I-shape reflector showed similar values. The spectral geometry-based DF results in higher thermal flux and lower fast flux at the interface compared to the 2D whole-core DF. This spectral distortion introduces discrepancies in nodal calculations, affecting reactivity behavior.

Table 2. Surface flux (#/cm²·s) and DF for L-shape reflector

		Spectral geometry		Whole-core	
ϕ_{fast}	Het.	4.0167E+13	3.9243E+13	2.6152E+12	2.2753E+12
	Hom.	3.8966E+13	3.8055E+13	2.8152E+12	2.4338E+12
ϕ_{th}	Het.	3.4741E+12	3.3147E+12	5.2929E+09	4.7821E+09
	Hom.	3.7485E+12	3.5676E+12	8.3393E+09	6.8632E+09
DF	Fast	**1.0308**	**1.0312**	**0.9290**	**0.9349**
	Thermal	**0.9268**	**0.9291**	**0.6347**	**0.6968**

Figure 9 compares reactivity over EFPD for both DF models. The spectral geometry DF results in higher reactivity than the 2D whole-core DF due to its simplified modeling.

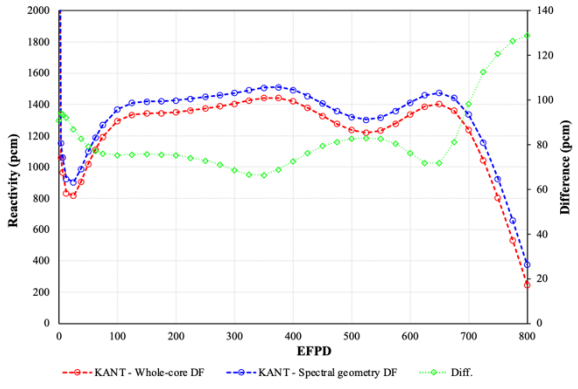

Figure 9. Reactivity comparison using different DF

The spectral geometry DF, while computationally efficient, introduces reactivity errors due to its simplified modeling. Conversely, the 2D whole-core DF offers improved accuracy at the cost of greater computational demand, highlighting a trade-off between efficiency and accuracy.

3.3 Monte Carlo and Two-step solution comparison

The accuracy of the two-step diffusion solution was assessed against the Monte Carlo reference solution. Figure 10 shows the reactivity comparison over EFPD, where deviations remain within 120 pcm throughout burnup, demonstrating reasonable agreement. Figure 11 presents the axial power distributions at the Beginning of Cycle (BOC) and End of Cycle (EOC), confirming that the two-step solution closely follows the Monte Carlo reference solution.

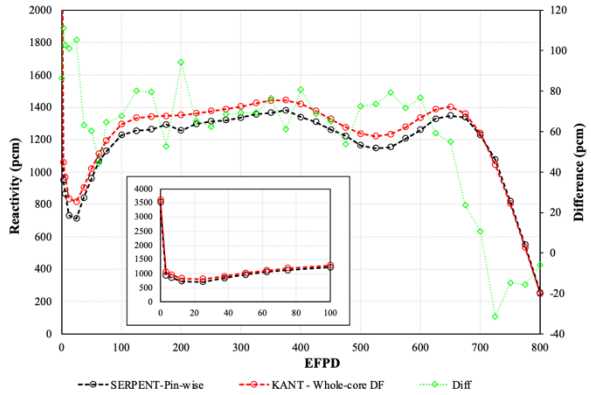

Figure 10. Reactivity comparison between Monte Carlo and two-step solutions

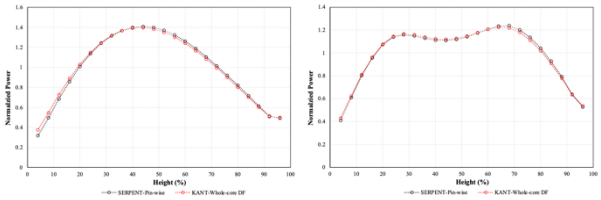

Figure 11. Axial power distribution comparision between SERPENT and KANT at BOC (left) and EOC (right)

BOC				
1.09	1.11	1.20	1.17	0.90
1.07	1.09	1.18	1.17	0.92
-1.63	-1.50	-0.96	0.14	2.94
1.11	1.11	1.13	1.13	0.81
1.09	1.10	1.12	1.13	0.83
-1.50	-1.37	-1.21	0.23	2.19
1.19	1.13	1.18	1.07	0.64
1.18	1.12	1.18	1.07	0.64
-0.71	-0.95	-0.45	0.13	0.72
1.16	1.12	1.06	0.78	
1.17	1.13	1.07	0.77	
0.40	0.68	0.51	-1.38	
0.90	0.81	0.64		SERPENT
0.92	0.83	0.64		KANT
2.94	2.19	0.72		Rel. Error(%)

EOC				
1.20	1.19	1.18	1.11	0.86
1.20	1.20	1.19	1.12	0.85
0.54	0.52	0.52	0.73	-0.78
1.19	1.19	1.17	1.09	0.82
1.20	1.19	1.17	1.10	0.82
0.52	0.33	-0.07	0.58	-0.58
1.18	1.17	1.14	1.01	0.65
1.20	1.18	1.15	1.01	0.64
1.35	0.68	0.53	-0.02	-2.17
1.13	1.10	1.02	0.75	
1.13	1.10	1.01	0.73	
0.48	0.26	-0.71	-2.93	
0.86	0.82	0.65		SERPENT
0.86	0.82	0.64		KANT
-0.38	-0.58	-2.17		Rel. Error(%)

Figure 11. Radial power distirubution comparision between SERPENT and KANT at BOC (left) and EOC (right)

4. Conclusions

This study established a Monte Carlo whole-core reference solution for a Soluble-Boron-Free i-SMR core and evaluated the two-step diffusion method. Spatial modeling approaches in Monte Carlo depletion significantly impacted reactivity, with fully pin-wise depletion providing the highest accuracy but at a high computational cost. Fuel rod grouping offered a practical alternative, balancing efficiency and accuracy.

The analysis also examined the impact of discontinuity factor modeling. While the spectral geometry DF provided computational efficiency, its simplified geometry altered neutron flux and DF values at the reflector interface, leading to deviations in reactivity calculations. In contrast, the 2D whole-core DF better preserved spectral fidelity, improving agreement with the reference solution. Despite inherent approximations, the two-step method demonstrated reasonable accuracy, maintaining reactivity deviations within 120 pcm and achieving close agreement in power distributions.

These findings highlight the necessity of appropriate fuel rod modeling strategies and accurate discontinuity factor for reliable nodal diffusion calculations, particularly in i-SMR employing HIGA as a burnable absorber.

ACKNOWLEDGEMENTS

This work was supported by the Innovative Small Modular Reactor Development Agency grant funded by the Korea Government RS-2024-00405419.

REFERENCES

[1] J. S. Kim, T. S. Jung, and J. Yoon, “Reactor core design with practical gadolinia burnable absorbers for soluble boron-free operation in the innovative SMR,” *Nuclear Engineering and Technology*, vol. 56, no. 8, pp. 3144–3154, Aug. 2024.

[2] J. Leppänen, M. Pusa, T. Viitanen, V. Valtavirta, and T. Kaltiaisenaho, “The Serpent Monte Carlo code: Status, development and applications in 2013,” Annals of Nuclear Energy, vol. 82, pp. 142–150, Aug. 2015.

[3] T. Oh, Y. Jeong, H. Khalefih, and Y. Kim, “Development and validation of multiphysics PWR core simulator KANT,” Nuclear Engineering and Technology, vol. 55, no. 6, pp. 2230–2245, Jun. 2023.

[4] A. E. Isotalo and P. A. Aarnio, “Higher order methods for burnup calculations with Bateman solutions,” Annals of Nuclear Energy, vol. 38, no. 9, pp. 1987–1995, Sep. 2011.